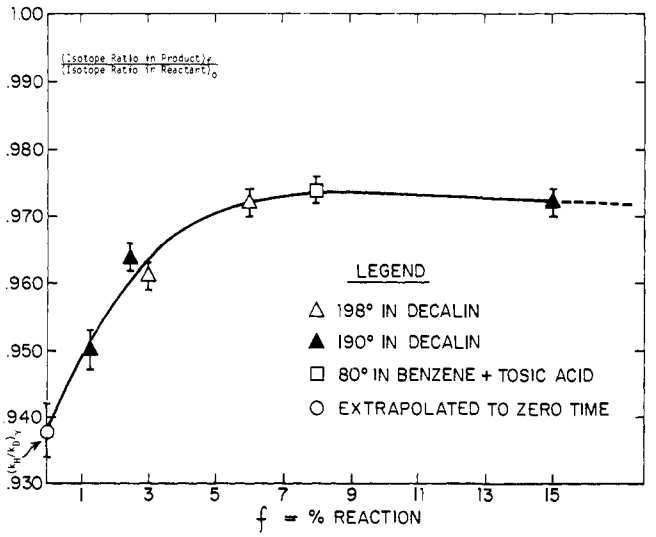

Figure 1.

then undergoes the same associative rearrangement mechanism as the purely thermal process.[17]

Acid catalysis of the thia-allylic rearrangement has also been observed by others.[10,18] The mechanism advanced,[10] namely, dissociation to an allyl cation following protonation of the central sulfur, is susceptible to the secondary deuterium isotope test. When an ~50:50 mix of **4** and **1** was rearranged in a degassed benzene solution containing tosic (*p*-toluenesulfonic) acid at 80 °C, the $(k_H/k_D)_\gamma$ value was virtually identical with that obtained for the uncatalyzed reaction (see Figure 1). This result renders an allylic cation intermediate[10] untenable. Furthermore, it reinforces the concept[1,8,15,19] that all thia-allylic rearrangements proceed through octet expansion of sulfur in various states of hypervalency, some created through the agency of catalysis[15,19] involving some form of coordination of sulfur by the catalytic species.

A pertinent case in point is concerned with the proposal[20] of a concerted, pseudopericyclic process of thia-allylic rearrangement of the allylic sulfide, represented by **9**. Thus, the

9

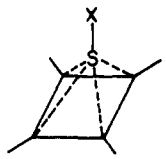

10

rapid isomerization reaction, which is detected by fluctional behavior in the NMR has been justified by quantum mechanical considerations.[21] This picture was preferred to an associative intermediate **10** with permutational isomerism, arising out of the octet-expanding abilities of the central sulfur. At first glance **10** might appear to involve an intolerable degree of strain. We submit, however, that this square pyramid (sp) structure, though bound at each of its basal vertices, is made more credible as an isomerization intermediate by the evidence presented here in support of the thiacyclobutane structure **6** in the usual thia-allylic process. Moreover, the ~12-kcal lowering of the activation energy for automerization[20,21] in **9** occasioned by the change from sulfide to sulfoxide (X = lone pair to X = oxygen) is made more understandable as a consequence of the lowering of the barrier to pseudorotation associated with increased hypervalency of the sulfur.[22] If the unshared pairs on sulfur played a decisive role in the automerization process, as postulated[20,21] in the pseudopericyclic rearrangement mechanism, this large activation energy difference is not easily explained.

References and Notes

(1) H. Kwart and J. J. Stanulonis, *J. Am. Chem. Soc.*, **98**, 4009 (1976).
(2) H. Kwart and N. A. Johnson, *J. Am. Chem. Soc.*, **92**, 6064 (1970).
(3) See J. C. Martin and T. M. Balthazor, *J. Am. Chem. Soc.*, **99**, 152 (177), for a discussion of the real geometries of species which ideally have TBP or SP structures distorted by bonding and other influences.
(4) See, for a survey of the general applicability of this criterion of mechanism, V. J. Shiner, Jr., in "Isotope Effects in Chemical Reaction", C. J. Collins and N. S. Bowman, Ed., Van Nostrand–Rheinhold, Princeton, N.J., 1971.
(5) W. A. Sheppard, R. F. W. Bader, and A. N. Bourns, *Can. J. Chem.*, **32**, 345 (1954); J. Bigeleisen, *Science*, **110**, 14 (1949).
(6) A. Streitwieser, Jr., R. H. Jagow, R. C. Fahey, and S. Suzuki, *J. Am. Chem. Soc.*, **80**, 2326 (1958).
(7) J. E. Baldwin and J. A. Kapecki, *J. Am. Chem. Soc.*, **92**, 4874 (1970).
(8) (a) H. Kwart and N. A. Johnson, *J. Am. Chem. Soc.*, **99**, 3441 (1977). (b) A referee has kindly pointed out that this result is comparable with the secondary deuterium isotope effect observed in the solvolysis of cyclobutyl-α-*d* mesylate. It is generally believed that the small effect (k_H/k_D = 1.10) in this case is a consequence of C_1–C_3 bonding developed in forming a bicyclobutonium ion intermediate. The zwitterionic nature of the "thia-cyclobutyl" intermediate in the thia-allylic rearrangement enhances this

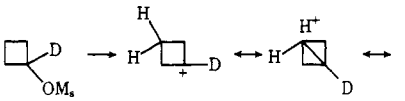

interaction and is to be held responsible for the large inverse effect observed.
(9) W. A. Pryor, R. W. Henderson, R. A. Patsiga, and N. Carrol, *J. Am. Chem. Soc.*, **88**, 1199 (1966).
(10) P. Brownbridge and S. Warren, *J. Chem. Soc., Perkin Trans. 1*, 2125 (1976).
(11) P. J. Krusic and J. K. Kochi, *J. Am. Chem. Soc.*, **93**, 846 (1971).
(12) E. S. Huyser and R. M. Kellog, *J. Org. Chem.*, **30**, 2867 (1965).
(13) S. N. Lewis, J. J. Miller, and S. Winstein, *J. Org. Chem.*, **37**, 1478 (1972).
(14) S. J. Cristol and R. Kellman, *J. Org. Chem.*, **36**, 1866 (1971).
(15) H. Kwart and N. A. Johnson, unpublished work.
(16) Unpublished results from these laboratories to be presented in a future article.
(17) E. F. Ullman, *Acc. Chem. Res.*, **1**, 353 (1968).
(18) P. Brownbridge and S. Warren, *J. Chem. Soc., Chem. Commum.*, 820 (1975).
(19) H. Kwart, N. A. Johnson, T. Eggerichs, and T. J. George, *J. Org. Chem.*, **42**, 172 (1977).
(20) C. H. Bushweller, J. A. Ross, and D. M. Lemal, *J. Am. Chem. Soc.*, **99**, 629 (1977).
(21) J. A. Ross, R. P. Seiders, and D. M. Lemal, *J. Am. Chem. Soc.*, **98**, 4325 (1976).
(22) Unpublished results of D. Benko from these laboratories indicate that aryl allyl sulfoxides undergo thia-allylic rearrangement by a process analogous to that experienced by aryl allyl sulfides.

Harold Kwart,* Thomas J. George
Department of Chemistry, University of Delaware
Newark, Delaware 19711

Received February 24, 1977

Anomalously Intense Raman Spectra of Pyridine at a Silver Electrode

Sir:

Raman spectra of pyridine adsorbed at a silver electrode which had previously been roughened by repeated electrochemical cycling have already been reported by Hendra and coworkers.[1,2] The purpose of this communication is to report that the Raman spectra of pyridine at a silver electrode, after a single oxidation-reduction cycle and particularly when recorded during and immediately after the cycle, are remarkably and anomalously intense. As an indication of the extent of this intensity enhancement the Raman signals that we observed from the ring-stretching modes of surface pyridine were roughly five times the corresponding signals from pure liquid pyridine in a conventional multipass optical cell, and they saturated the detection system of our spectrometer for an incident laser power of only 15 mW (514.5 nm) and 4-cm^{-1} slits! The resulting high signal/noise ratio enables the intensities of bands due to pyridine at different types of surface site to be readily measured. This letter thus also presents preliminary results on the variation in intensity of the 1025-cm^{-1} band of

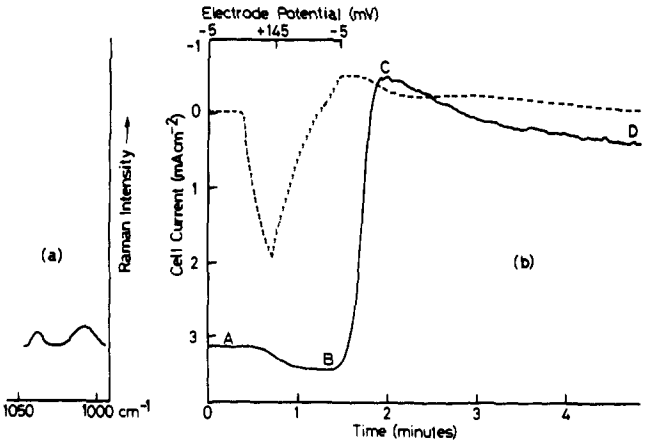

Figure 1. (a) Raman spectrum of a freshly cleaned silver electrode at the open-circuit potential immersed in an aqueous solution 10^{-2} M in pyridine and 10^{-1} M in KCl. Laser power (514.5 nm) = 100 mW. (b) Variation (—) of the total signal at $\Delta\nu$ 1025 cm^{-1} and cell current (- - -) accompanying the application of a triangular waveform to the electrode. Laser power = 9 mW, same intensity scale as for a.

adsorbed pyridine plotted simultaneously with a voltammogram, which demonstrate the considerable potential of Raman spectroscopy for monitoring electrochemical processes at this electrode at a molecular level.

An electrochemical cell similar to the one used by Hendra[1] was controlled by a potentiostat and waveform generator. The "Specpure" silver was supplied by Johnson Matthey. All other chemicals were A.R. grade, and solutions were prepared with triply distilled water. The 514.5-nm laser radiation was directed onto the electrode at near-grazing incidence. The scattered radiation was collected at 90° by a Coderg PH1 Raman spectrometer with EMI 9558A phototube and DC detection. The electrode was cleaned by abrading with sandpaper and then washing in triply distilled water. All electrode potentials were measured and are quoted with respect to a saturated calomel electrode.

In Figure 1a is shown a part of the Raman spectrum of a freshly cleaned silver electrode immersed in a solution 10^{-2} M in pyridine and 10^{-1} M in KCl. We believe from control experiments in which the electrode was withdrawn from the laser beam that these bands owe most of their intensity to pyridine in the bulk electrolyte, and the 1025-cm^{-1} band attributed by Hendra et al. to Lewis-coordinated pyridine is clearly absent prior to electrochemical treatment of the electrode. Figure 1b shows the change in total signal at $\Delta\nu$ 1025 cm^{-1} accompanying the application of a single triangular voltage sweep to the electrode from −5 to +145 mV and back to a final and maintained value of −5 mV. The sweep speed was 3.4 mV s^{-1}. The drop in signal at A (Figure 1b) is due to a decrease in the background stray-light intensity resulting from a change in surface texture and darkening of the electrode during anodization, and throughout the anodic sweep the 1025-cm^{-1} band is absent from the spectra. At the start of the cathodic sweep and coincident with the reduction of AgCl (B, Figure 1b) the 1025-cm^{-1} band rises sharply and then decays, continuing to do so after completion of the voltage sweep, until it reaches a constant value at D. Stopping the sweep at a more negative potential, which increases the final overpotential for silver chloride reduction, increases the decay rate between C and D. Other bands characteristic of surface pyridine at 1008, 1036, 1218, and 1605 cm^{-1} showed similar but not identical intensity changes. Thus Figure 2 shows Raman spectra of adsorbed pyridine in the region 1000–1050 cm^{-1} at selected stages of the oxidation-reduction cycle and immediately thereafter, which show changes in the relative intensities of bands consistent with the steady-state spectra of Hendra et al.[1]

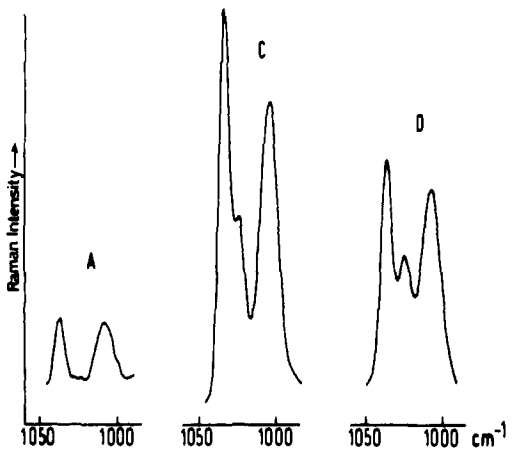

Figure 2. Raman spectra of absorbed pyridine ($\Delta\nu$ 1000–1050 cm^{-1}) recorded around A, C, and D of Figure 1b (spectrum A, ×10).

For electrode potentials less than −1.0 V the spectrum resembles that of solution pyridine (Figure 1a) both in frequencies and intensities, and the bands of adsorbed pyridine are not restored on returning to the potential of zero charge (−0.71 V)[3] without first anodizing the electrode surface.

The increase in surface area resulting from a single cyclic voltage sweep can be estimated from the results of Katan et. al.[4] who used a scanning electron microscope to study the surface morphology of silver electrodes subjected to a similar treatment. Pit formation was observed by them at a surface density of $\sim 1.8 \times 10^8$ cm^{-2} with an average pit cross section of 300 nm. Estimating the pit depth to be 100–200 nm, comparable with the thickness of deposited AgCl, leads to an increase in surface area of only 10–20%. The oxidation-reduction treatment does not therefore appear to be associated with a sufficient growth in surface area to produce the large increase in the amount of surface pyridine necessary to explain the increase in Raman signal during the cathodic sweep. It was noted above that the Raman bands of surface pyridine after the oxidation-reduction cycle are roughly five times as intense as the bands of pure liquid pyridine in a conventional optical cell, even though estimates based on the isotherm of Barradas and Conway[5] with an assumed surface roughness factor of 3.5 show that scattered light is collected from roughly 4×10^5 times as many molecules in the pure liquid pyridine sample than at the electrode surface. We are thus led to conclude that there is a considerable enhancement ($\sim \times 10^5$) in the spectra of the adsorbed pyridine by a surface effect which greatly increases the molecular Raman scattering cross sections. It has been suggested by Philpott[6] that broadening of the electronic energy levels of molecules at roughened metal surfaces may induce resonant Raman scattering from molecules adsorbed on metals through interaction with surface plasmons. Resonant Raman enhancements of the order of 10^5 and above are certainly known for some conjugated chromophores,[7] and it may prove that this is the explanation of the intensity enhancement reported here. We have, however, so far been unable to observe the intense progressions of overtones characteristic of resonant Raman scattering, nor any marked difference in the enhancement on changing from 514.5- to 632.8-nm excitation, and we have thus no evidence to confirm this explanation at present.

Detailed studies of this and related electrode systems are in progress and will be published shortly.

Acknowledgment. We acknowledge a research grant from the Ministry of Defence.

References and Notes

(1) M. Fleishmann, P. J. Hendra, and A. J. McQuillan, *Chem. Phys. Lett.*, **26**, 163 (1964).

(2) A. J. McQuillan, P. J. Hendra, and M. Fleischmann, *J. Electroanal. Chem.* **65**, 933 (1975).
(3) W. Palk, M. A. Genshaw and J. O'M. Bockris, *J. Phys. Chem.*, **74**, 4266 (1970).
(4) T. Katan, S. Szpak, and D. N. Bennion, *J. Electrochem. Soc.*, **121**, 757 (1974).
(5) R. G. Barradas and B. E. Conway, *J. Electroanal. Chem.*, **6**, 314 (1963).
(6) M. R. Philpott, *J. Chem. Phys.*, **62**, 1812 (1975).
(7) J. Behringer, "Raman Spectroscopy", Vol. 1, H. A. Szymanski, Ed., Plenum Press, New York, N.Y., 1967, pp 168–223.

M. Grant Albrecht, J. Alan Creighton*
The Chemical Laboratory
University of Kent at Canterbury, Kent, England
Received April 15, 1977

Structure of the Catalytic Site of Polymer-Bound Wilkinson's Catalyst by X-Ray Absorption Studies

Sir:

Recently, there has been considerable interest in linking homogeneous catalysis to heterogeneous catalysis by using insoluble organic polymers as supports for transition metal catalysts.[1] Polymer-bound Wilkinson's catalyst,[2] $(Ph_3P)_3RhCl$, has been investigated[3] as a hydrogenation catalyst where the supporting medium is polystyrene cross-linked with divinylbenzene. Despite Collman et al.'s[4] work on $RhClL_3$ (where L = cross-linked polystyrene-*p*-C_6H_4-PPh_2), the detailed structures of these heterogenized homogeneous catalysts[5] remain essentially unknown.

We report herein the interatomic distances and coordination of Wilkinson's catalyst (red isomer,[2,6] (**1**)), polymer-bound Wilkinson's catalyst[3] (**2**), and hydrogenated polymer-bound Wilkinson's catalyst[7] (**3**) as determined by x-ray absorption studies performed with synchrotron radiation at the Stanford Synchrotron Radiation Project.[8-13] This technique has been used to measure internuclear distances in iron-sulfur proteins,[14] copper salts in aqueous solutions,[12] and various molecules.[15,16]

It has been shown,[17-22] that the modulation $\Delta\mu$ of the x-ray absorption coefficient of an atom is given by

$$\chi(k) = \frac{\Delta\mu}{\mu} = \sum_j \frac{-N_j|f_j(k,\pi)|e^{-2\sigma_j^2k^2}}{R_j^2k} \sin\,[2kR_j + \phi_j(k)] \tag{1}$$

where N_j is the number of scattering atoms j at a distance R_j to the absorbing atom with a Debye-Waller-like factor $e^{-2\sigma_j^2k^2}$.[23] The $\phi_j(k)$ and $f_j(k,\pi)$ are energy-dependent phase-shift and electron back-scattering form factor. The k wave vector of the emitted photoelectron is given by

$$k = \sqrt{2m(E - E_{th})/\hbar^2} \tag{2}$$

where E_{th} is the absorption threshold energy for the atom. $\phi_j(k)$ depends upon the absorbing and the neighboring atoms whereas $f_j(k,\pi)$ depends only on the neighboring atom j.[19] Thus, above threshold, one observes (Figure 1) a sinusoidal variation of the x-ray absorption in which the frequency depends on R_j and $\phi_j(k)$ and the amplitude depends on N_j, σ_j, and $f_j(k,\pi)$. In this work, we used model compounds $Rh(dppe)_2^+$ (dppe, diphenylphosphinoethane) and $RhCl_3 \cdot nH_2O$ to obtain $\phi_j(k)$ and $f_j(k,\pi)$ for Rh-P and Rh-Cl bonds.[19,24] To determine N_j and R_j for **1**, **2**, and **3** the Fourier filtered data which included only nearest neighbor contributions (the only predominant feature in the Fourier transform) were fitted to the function

$$\begin{aligned}\frac{\Delta\mu}{\mu} = {} & N_{P_1} \sin\,[2kR_{P_1} + \phi_P(k)]f_P(k)e^{-2\sigma_{P_1}^2k^2} \\ & + N_{P_2} \sin\,[2kR_{P_2} + \phi_P(k)]f_P(k)e^{-2\sigma_{P_2}^2k^2} \\ & + N_{Cl} \sin\,[2kR_{Cl} + \phi_{Cl}(k)]f_{Cl}(k)e^{-2\sigma_{Cl}^2k^2}\end{aligned} \tag{3}$$

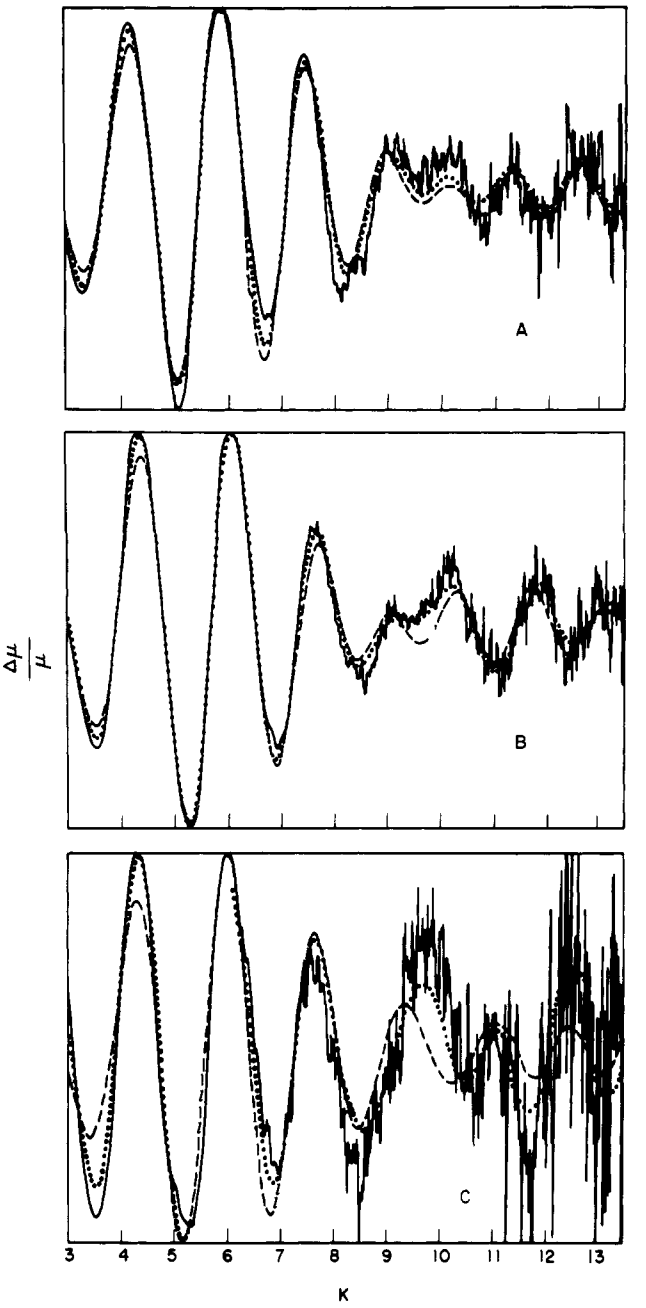

Figure 1. Raw (—), Fourier filtered (• • •) and fit (- - -) of data, multiplied by k^3: A, $(PPh_3)_3RhCl$; B, polymer-bound $(PPh_3)_3RhCl$; C, hydrogenated polymer-bound $(PPh_3)_3RhCl$.

The results of the fitting procedure are summarized in Table I. The significant phase shift difference (~0.5 rad) between $\phi_P(k)$ and $\phi_{Cl}(k)$ enables one to distinguish between phosphorus and chlorine contributions.[19] This fitting technique[24] also gave information about the number of phosphorus vs. chlorine (scatterers) atoms attached to the rhodium (absorber) atom. In Figure 2 the sum of the squares of the fit residuals (χ^2) is plotted for several values of $N_P = N_{P_1} + N_{P_2}$ and N_{Cl}. In this fit of the data only integral N_{P_1}, N_{P_2}, and N_{Cl} values were considered.

The interatomic distances (cf. Table I) in **1** are: Rh-Cl, 2.35, one short Rh-P_1 of 2.23, and two long Rh-P_2 of 2.35 Å, which are in agreement with those determined by x-ray crystallography.[6] Furthermore, our result (cf. curve A in Figure 2) clearly shows that the best fit occurs at P:Cl ratio of 3:1 (viz., 1:2:1 N_{P_1}:N_{P_2}:N_{Cl}).

The distances found for **2** showed the loss of the two long